

2

NAVAL POSTGRADUATE SCHOOL

Monterey, California

AD-A167 714



DTIC
ELECTE
MAY 21 1986
S D E

THESIS

EXPERIMENTAL PROCEDURE FOR LIFETIME TESTING OF
GRAPHITE BUNDLES UNDER CONSTANT LOAD

by

Fred D. Carozzo, Jr.

March 1986

Thesis Advisor:

Edward M. Wu

Approved for public release; distribution is unlimited

DTIC FILE COPY

REPORT DOCUMENTATION PAGE

1a. REPORT SECURITY CLASSIFICATION UNCLASSIFIED		1b. RESTRICTIVE MARKINGS	
2a. SECURITY CLASSIFICATION AUTHORITY		3. DISTRIBUTION/AVAILABILITY OF REPORT Approved for public release; distribution is unlimited.	
2b. DECLASSIFICATION/DOWNGRADING SCHEDULE		5. MONITORING ORGANIZATION REPORT NUMBER(S)	
4. PERFORMING ORGANIZATION REPORT NUMBER(S)		7a. NAME OF MONITORING ORGANIZATION Naval Postgraduate School	
6a. NAME OF PERFORMING ORGANIZATION Naval Postgraduate School	6b. OFFICE SYMBOL (if applicable)	7b. ADDRESS (City, State, and ZIP Code) Monterey, California 93943-5100	
6c. ADDRESS (City, State, and ZIP Code) Monterey, California 93943-5100		9. PROCUREMENT INSTRUMENT IDENTIFICATION NUMBER	
8a. NAME OF FUNDING/SPONSORING ORGANIZATION	8b. OFFICE SYMBOL (if applicable)	10. SOURCE OF FUNDING NUMBERS	
8c. ADDRESS (City, State, and ZIP Code)		PROGRAM ELEMENT NO.	PROJECT NO.
		TASK NO.	WORK UNIT ACCESSION NO.
11. TITLE (Include Security Classification) EXPERIMENTAL PROCEDURE FOR LIFETIME TESTING OF GRAPHITE BUNDLES UNDER CONSTANT LOAD			
12. PERSONAL AUTHOR(S) Carozzo, Jr. Fred D.			
13a. TYPE OF REPORT Master's Thesis	13b. TIME COVERED FROM TO	14. DATE OF REPORT (Year, Month, Day) 1986 March	15. PAGE COUNT 50
16. SUPPLEMENTARY NOTATION			
17. COSATI CODES		18. SUBJECT TERMS (Continue on reverse if necessary and identify by block number)	
FIELD	GROUP	Composite, Graphite Fibers, Creep Rupture.	
		Viscoelastic Deformation, Fiber life.	
19. ABSTRACT (Continue on reverse if necessary and identify by block number)			
<p>An experimental procedure is presented for lifetime testing of graphite bundles under constant load. The attributes of the experiment are expedience in implementation and a substantial accumulation of information equivalent to a large number of single filament tests. To achieve the objectives of the experiment a specially adapted Instron machine was used with a digital process/controller. Two trial experiments were conducted using Hercules high strength graphite. The preliminary results are presented and the effects of inter-fiber friction evaluated.</p>			
20. DISTRIBUTION/AVAILABILITY OF ABSTRACT <input checked="" type="checkbox"/> UNCLASSIFIED/UNLIMITED <input type="checkbox"/> SAME AS RPT. <input type="checkbox"/> DTIC USERS		21. ABSTRACT SECURITY CLASSIFICATION UNCLASSIFIED	
22a. NAME OF RESPONSIBLE INDIVIDUAL Edward M. Wu		22b. TELEPHONE (Include Area Code) (408) 646-2944	22c. OFFICE SYMBOL 67

Approved for public release; distribution is unlimited.

Experimental Procedure for Lifetime Testing
of Graphite Bundles Under Constant Load

by

Fred D. Carozzo, Jr.
Lieutenant, United States Navy
B.S., University of Nebraska-Lincoln, 1978

Submitted in partial fulfillment of the
requirements for the degree of


MASTER OF SCIENCE IN AERONAUTICAL ENGINEERING

from the

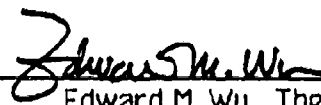
NAVAL POSTGRADUATE SCHOOL

March 1986

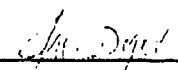
Author:


Fred D. Carozzo, Jr.

Approved by:


Edward M. Wu, Thesis Advisor


Max F. Platzer, Chairman, Department of Aeronautics


John N. Dyer, Dean of Science and Engineering

ABSTRACT

An experimental procedure is presented for lifetime testing of graphite bundles under constant load. The attributes of the experiment are expedience in implementation and a substantial accumulation of information equivalent to a large number of single filament tests. To achieve the objectives of the experiment a specially adapted Instron machine was used with a digital process/controller. Two trial tests were conducted using Hercules high strength graphite. The preliminary results are presented and the effects of inter-fiber friction evaluated.

Accession For	
NTIS GRA&I	<input checked="checked" type="checkbox"/>
DTIC TAB	<input type="checkbox"/>
Unannounced	<input type="checkbox"/>
Justification	
By	
Distribution/	
Availability Codes	
Dist	Avail and/or Special
A-1	



TABLE OF CONTENTS

I.	INTRODUCTION	7
II.	BACKGROUND	9
	A. FIBER STRENGTH	9
	B. FIBER LIFETIME	11
	C. COMPOSITE LIFETIME	13
III.	EXPERIMENTAL METHOD	17
	A. MATERIALS AND PREPARATION	17
	B. EQUIPMENT AND INSTRUMENTATION	18
	C. DATA ACQUISITION	25
	D. TESTING PROCEDURE	26
IV.	RESULTS	29
V.	CONCLUSIONS AND RECOMMENDATIONS	34
	A. CONCLUSIONS	34
	B. RECOMMENDATIONS	34
	APPENDIX A: PROGRAM LISTINGS	35
	APPENDIX B: GRAPHICAL RESULTS	40
	LIST OF REFERENCES	47
	BIBLIOGRAPHY	48
	INITIAL DISTRIBUTION LIST	49

LIST OF FIGURES

3.1	Alcohol Rinse Setup	19
3.2	Copper Tube to Produce Laminar Flow	20
3.3	Holders and Jig for Sample Preparation	20
3.4	Block Diagram of Experimental Setup	21
3.5	IMC Digital Processor/Controller	23
3.6	Crosshead with Load Transducer	24
3.7	Instron Universal Testing Instrument	27
3.8	Differential Screw Mechanism	28
A.1	Modified HP44468A Data Logger Routine	35
A.2	Modified HP44468A Output Format Routine	39
B.1	Test 1: Load Time Curves	40
B.2a	Test 2: Load Time Curves	41
B.2b	Test 2: Load Time Curves	42
B.3	Test 1: Normalized Load Curves	43
B.4	Test 2: Normalized Load Curves	44
B.5	Test 1: Life Distribution Curve	45
B.6	Test 2: Life Distribution Curve	46

ACKNOWLEDGMENTS.

To Professor Edward M. Wu for his guidance and patience, and the many helpful discussions. To Ted Dutton for his invaluable assistance and understanding, and to Bob Besel for his technical advice and time taken in procuring all the required hardware.

I. INTRODUCTION

Composite materials have been used by man for a very long time. The first to be used were naturally occurring composites, such as wood. Then man discovered that there were advantages to be gained by combining materials with one component being fibrous, such as the use of straw to strengthen mud bricks. More recently, fiber reinforced composites with polymer and metal binder that have high strength to weight and high stiffness to weight ratios have become important in applications such as aircraft and space vehicles.

In the 1960's the U.S. Air Force began programs to explore aircraft structures made of composites. The first flight-worthy component produced was the horizontal stabilizer for the F-111. Another major milestone was the production of a composite stabilizer for the F-14. That was followed by the composite stabilator for the F-15, and a composite rudder and stabilizer for the F-16. [Ref. 1]

The advantages of composites when compared to conventional materials is that they exhibit the best qualities of their constituents and sometimes qualities that neither constituent possesses. Therefore, an understanding of reinforcement processes together with failure mechanisms is important for the development and production of high quality composites and for forecasting the long term stability of such structures, particularly in high performance applications.

The purpose of this thesis is to present an experimental procedure for lifetime testing of graphite bundles under constant load for use in forecasting the life of graphite composite structures. And to demonstrate by comparison to single filament data that composite life is bracketed by composite load-sharing life as the upper bound, and fiber life as the lower bound.

II. BACKGROUND

A. FIBER STRENGTH

Brittle fibers used as reinforcement materials for advanced composites, such as carbon and glass, are characterized by high strength and high modulus, and have tensile strengths that are statistical rather than deterministic in nature. This statistical dispersion in strength is attributed to the existence of fiber surface defects.

Rosen [Ref. 2 and 3] presented the results of an analytical and experimental composite failure study. His theory considers fibers having a statistical distribution of flaws that result in individual fiber breaks at various stress levels. The load in a broken fiber is assumed to be distributed equally among the remaining unbroken fibers in a cross section. Composite failure is hypothesized to occur when the weakest cross section is unable to sustain the applied load.

In Rosen's model, the applied load is considered to be supported entirely by the fibers since their extensional modulus is much greater than that of the matrix. Because the fibers have randomly distributed flaws they break randomly throughout the length of the fiber as the load is increased. In the vicinity of a break, the fiber stress is redistributed by the matrix binder, limiting only a portion of the fiber not fully effective in resisting the applied load. By a logical extension of this reasoning, the composite can be thought of as consisting of a series of layers of elements, analogous to links in a chain, whose axial length is equal to the ineffective length δ .

The ineffective length which is a function of the fiber volume fraction can be expressed, based upon an elastic analysis, as

$$\delta = 1/2[(V_f^{-1/2} - 1)E_f/G_m]^{1/2} \cosh^{-1}\{[1 + (1 + \phi)^2]/2(1 - \phi)\}d_f \quad (1)$$

where V_f is the fiber volume fraction, E_f is the fiber Young's modulus, G_m is the matrix shear modulus, ϕ is the fraction of the undisturbed stress value below which the fiber is considered to be ineffective, and d_f is the fiber diameter [Ref. 4].

Although Rosen's model agrees qualitatively with experimental data, in that failure is associated with the accumulation of fiber breaks, there is a disparity between predicted and observed failure loads, due to the simplifying assumption that the load in a broken fiber is uniformly distributed among the other fibers in the layer.

Since it was logical to study the correlation between the theoretical strength of the weakest fiber and the observed failure loads, Rosen considered a population of fibers of length L whose strength is characterized by the probability density function $g(\sigma)$ and cumulative distribution function $G(\sigma)$. [Ref. 2 pp 68-71]

For a sample of n links, where $n = L/\delta$, the probability density function for the strength of the weakest fiber is given by

$$f(\sigma) = [g(\sigma)/n][1 - G(\sigma)]^{(1/n)-1} \quad (2)$$

It is assumed that the fiber strength can be characterized by a two parameter Weibull distribution of the form

$$G(\sigma) = 1 - \exp(-\alpha L \sigma^\beta) \quad (3)$$

which has a corresponding density

$$g(\sigma) = \alpha L \beta \sigma^{\beta-1} \exp(-\alpha L \sigma^\beta) \quad (4)$$

With $L = \delta$, and substituting equation (3) and (4) into equation (2) and then differentiating, the desired expression is obtained for the statistical mode of the weakest fiber strength distribution which is

$$\sigma^* = V_f (\alpha \delta \beta e)^{-1/\beta} \quad (5)$$

The constants α and β denote the scale parameter and shape parameter of the Weibull distribution, respectively, and can be evaluated by using experimental strength-length data.

B. FIBER LIFETIME

Consider a bundle of stiff, brittle fibers impregnated with a flexible matrix. Suppose a constant, tensile load is applied such that the impregnated bundle, though surviving at first, fails after many hours. This type of

fracture is a thermally activated process, and is referred to as stress-rupture or creep rupture. As a thermally activated process, failure originates in the fibers where the molecules undergo random, thermal vibrations in time. As molecules slip or rupture, neighboring molecules become overloaded, thus increasing their failure rates. Such molecular failure accumulate locally and give rise to growing microcracks. These cracks eventually lead to broken fibers scattered throughout the composite. The randomness of these fiber breaks, both in position and time, is magnified by randomly distributed structural imperfections. [Ref. 5 pp 135-136]

Historically, various kinetic models have been proposed to explain the phenomena of creep-rupture. But none of those proposals dealt with the variability of the lifetime data, which is an important aspect of creep-rupture in composites.

Wagner [Ref. 6] presents the results of an analytical and experimental study for creep-rupture lifetime of Kevlar 49, fibers. The model, reflects fiber variability and sensitivity of lifetime to load level, based upon the logarithmic approximation

$$U(\sigma) = -U_0 \ln(\sigma/\sigma_0) \quad (6)$$

where $U(\sigma)$ the thermal activation energy to rupture an atomic bond is a function of molecular stress σ , the maximum bond force σ_0 , and the activation energy U_0 in the absence of stress. This approximating function

accounts for the power law relationship for the dependence of lifetime on stress level [Ref. 5].

The power law framework which is based on the thermal activation process of molecular failure generates the result that the fiber strength and fiber lifetime follow the Weibull distribution.

The Weibull distribution for fiber lifetime under constant stress is

$$F(t) = 1 - \exp\{-[t/t_1(\sigma)]^\beta\} \quad (7)$$

with shape parameter β and scale parameter

$$t_1(\sigma) = m^{-1/\beta} t_8(\sigma) \quad (8)$$

where $m = 1/\delta$ and

$$t_8(\sigma) = \sigma^{-[U_0/(kT)]/\gamma} \alpha^{1/\beta} \quad (9)$$

γ is a positive constant from the power law relationship.

C. COMPOSITE LIFETIME

As presented earlier, Rosen assumed the load in a broken fiber to be uniformly distributed among the other fibers in the layer which are intact. However, a more complex structure exists in the relationship between the

fiber and matrix. Which is, that the fibers adjacent to a broken one are subjected to a load intensity greater than that which is sustained by fibers distant from the fracture point. Phoenix and Wu [Ref. 5] describe this phenomena as local load sharing.

In local load sharing, the matrix serves two important functions: First, the effect of the fiber break is isolated longitudinally along the fiber as the shear stress in the matrix allows the fiber stress to return to normal a short axial distance away from the break. At the same time it permits the lateral transfer of the failed fiber load to its nearest neighbors. The increased loads on these neighbors greatly enhance their rate of failure. As these neighboring fibers break a transfer of the load continues until some unstable group of adjacent breaks, called a k^* -crack emerges, and suddenly propagates across the composite. [Ref. 5]

At high load levels, the shear in the matrix at fiber fractures may exceed the matrix mechanical properties causing cracks which propagate longitudinally as well as transversely. The ability of the composite to support high tensile loads is strongly influenced by the shear carrying ability of the matrix and by the ability of the fiber to sustain high tensile loads.

The mathematical model of the failure process presented by Phoenix and Wu is a weakest-link arrangement of independent bundles of length equal to the effective load transfer length δ which is given by equation (1).

In any given bundle the fiber elements share the applied load, which yields a nominal fiber stress. Since a failed element supports no stress, the stress of the failed element is redistributed onto its nearest neighbors, one on each side. An intact element next to one or more consecutive broken elements

carries a stress $K_r X$ which is expressed as

$$K_r = \pi(2_j + 2)/(2_j + 1), \quad j = 1, 2, \dots, r \quad (10)$$

where K_r is called the load concentration factor, X is the nominal fiber stress, and r is the number of consecutive broken fiber elements.

The distribution for composite lifetime has the Weibull approximation

$$H_{m,n}(t) \approx 1 - \exp\{-[t/t_c(L)]^{k^* \beta}\}, \quad t > 0 \quad (11)$$

with shape parameter $k^* \beta$ and scale parameter

$$t_c(L) = (mn)^{-1/(k^* \beta)} d_{k^*} t_g(L) \quad (12)$$

where d_{k^*} is given by

$$d_{k^*} = \Gamma(\beta + 1)^{-1/\beta} \Gamma(k^* \beta + 1)^{-1/(k^* \beta)} 2^{(1 - k^*)/(k^* \beta)} \pi(K_{j-1})^{-\rho/k^*} \quad (13)$$

The Weibull approximation given by equation (11), is valid for all values of $\beta \rho$ greater than 6, [Ref. 5 pp 141 - 142].

In these expressions the Weibull shape parameter and critical crack size varies with stress level, and account for the variability and size effect in strength and lifetime.

III. EXPERIMENTAL METHOD

A. MATERIALS AND PREPARATION

The fibrous material used to validate the experimental procedure to be presented was Hercules Magnamite high strength graphite with the following specifications:

Type	AS4 with W sizing
Tow	3000 filaments
Denier	0.005746 grams/inch
Diameter	7.0 microns

To prepare the samples for the experiment, 100 inches of fiber was layed out on a table. One end of the fiber was secured to the table while approximately 5 inches of the other end hung over the table edge with a 2 kilogram weight attached. A pulley at the edge, that the fiber layed over eliminated friction between the fiber and the table edge.

The 2 kilogram weight (approximately equal to 10% of the tow breaking load) was used to provide a small amount of tension and to ensure that all the filaments in each sample would be the same length when cut.

A smear, about an inch in length of Tru Bond 5 Minute Epoxy Gel was applied to the fiber every 15 inches. When the epoxy had cured the fiber was cut to produce six samples, each 15 inches in length, with one end of the sample coated with epoxy gel bonding its filaments together. Each sample was placed into a glass funnel that had a 10 inch exit tube, that protected the sample from damage during handling. Each funnel

with its sample was placed into a bath of methyl ethyl ketone for a period of twenty-four hours to remove the sizing, and then placed into an ethyl alcohol rinse (Figure 3.1) for one hour to flush away the residual sizing, and reduce random slack and disentangle the fibers. To prevent swirling of the alcohol through the funnel during the rinse, the copper tube (Figure 3.2) which delivered the alcohol into the funnel's mouth, was designed with perforations about its periphery. Immediately after the rinse while the sample was still wet, to take advantage of the surface tension of the fluid, holding the fibers together and straight, the free end of the sample was smeared with the epoxy gel. The sample remained in the funnel until the epoxy had cured.

Removed from the funnels, each sample was mounted onto one-half of its holder at each end (Figure 3.3) with epoxy. Before the epoxy cured, the mating half of the holder was bolted into place. This ensured that no slippage would occur within the holder. The gauge length used was 10 inches.

To determine if interfiber friction, after a fiber failure occurs is significant some of the samples were lubricated with silicone oil.

B. EQUIPMENT AND INSTRUMENTATION

The attributes of bundle testing are expedience in implementation and a substantial accumulation of information equivalent to a large number of single filament tests.

To achieve the objectives of the experiment it was necessary to be able to apply a constant stress to the test samples. Figure 3.4, depicts a

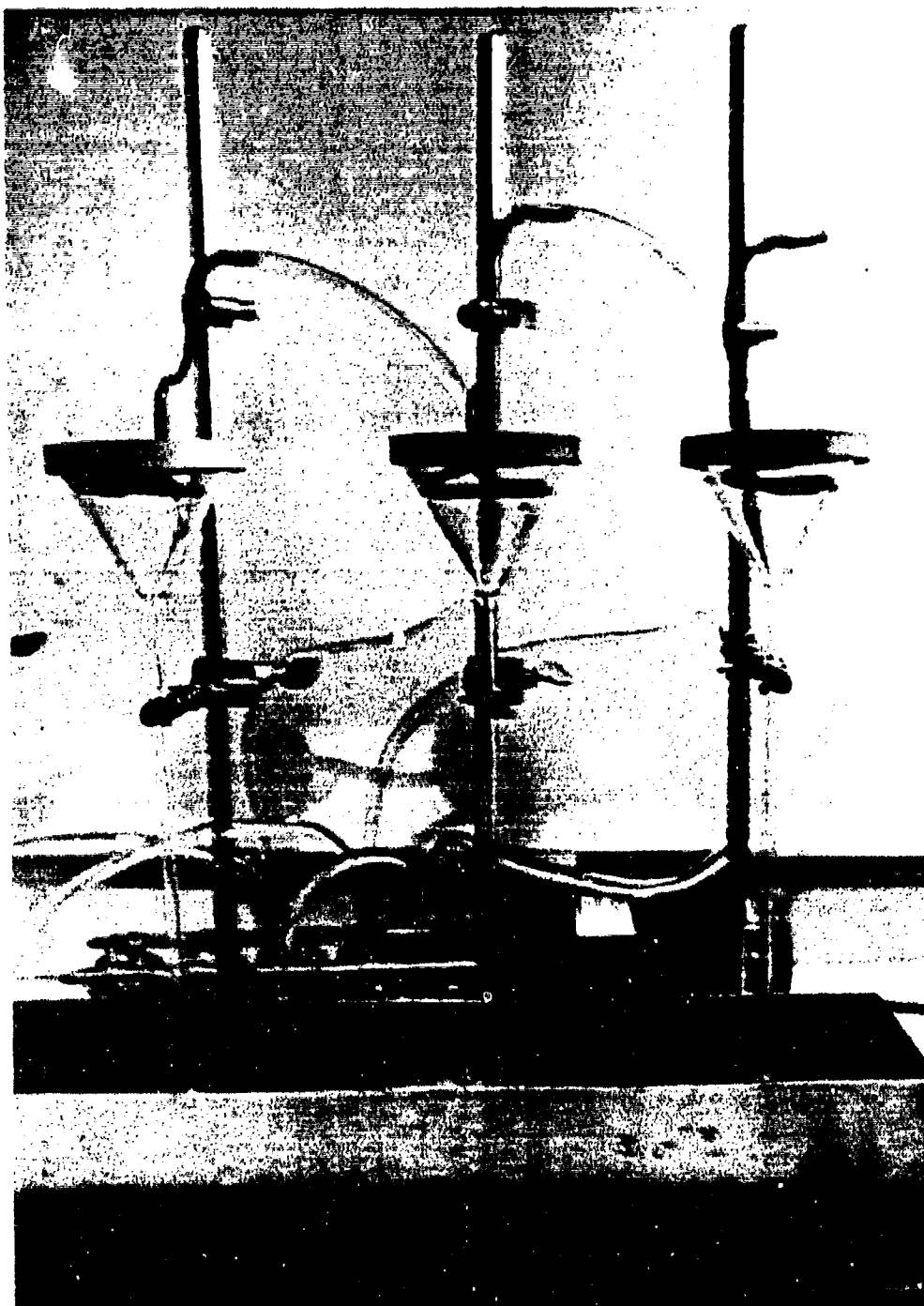


Figure 3.1. Alcohol rinse setup.

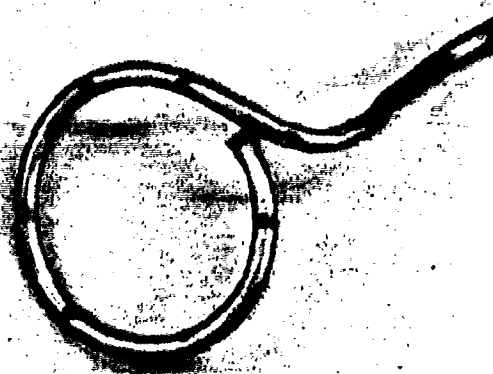


Figure 3.2. Copper tube designed to produce laminar flow.

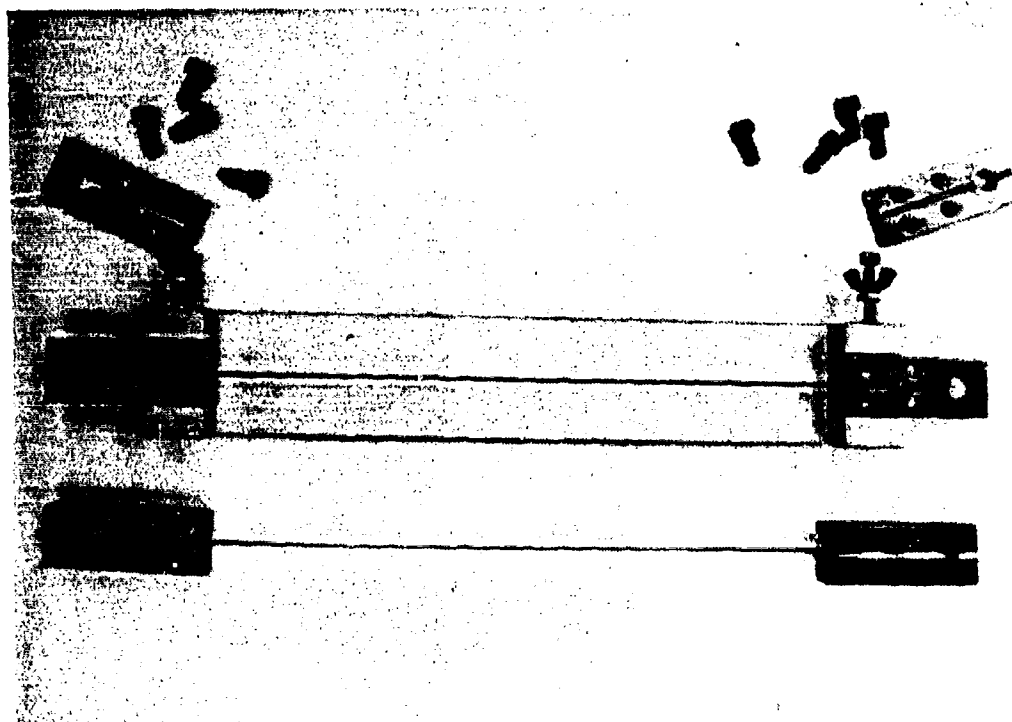


Figure 3.3. Holders shown in jig used to prepare samples. Gage length is 10 inches.

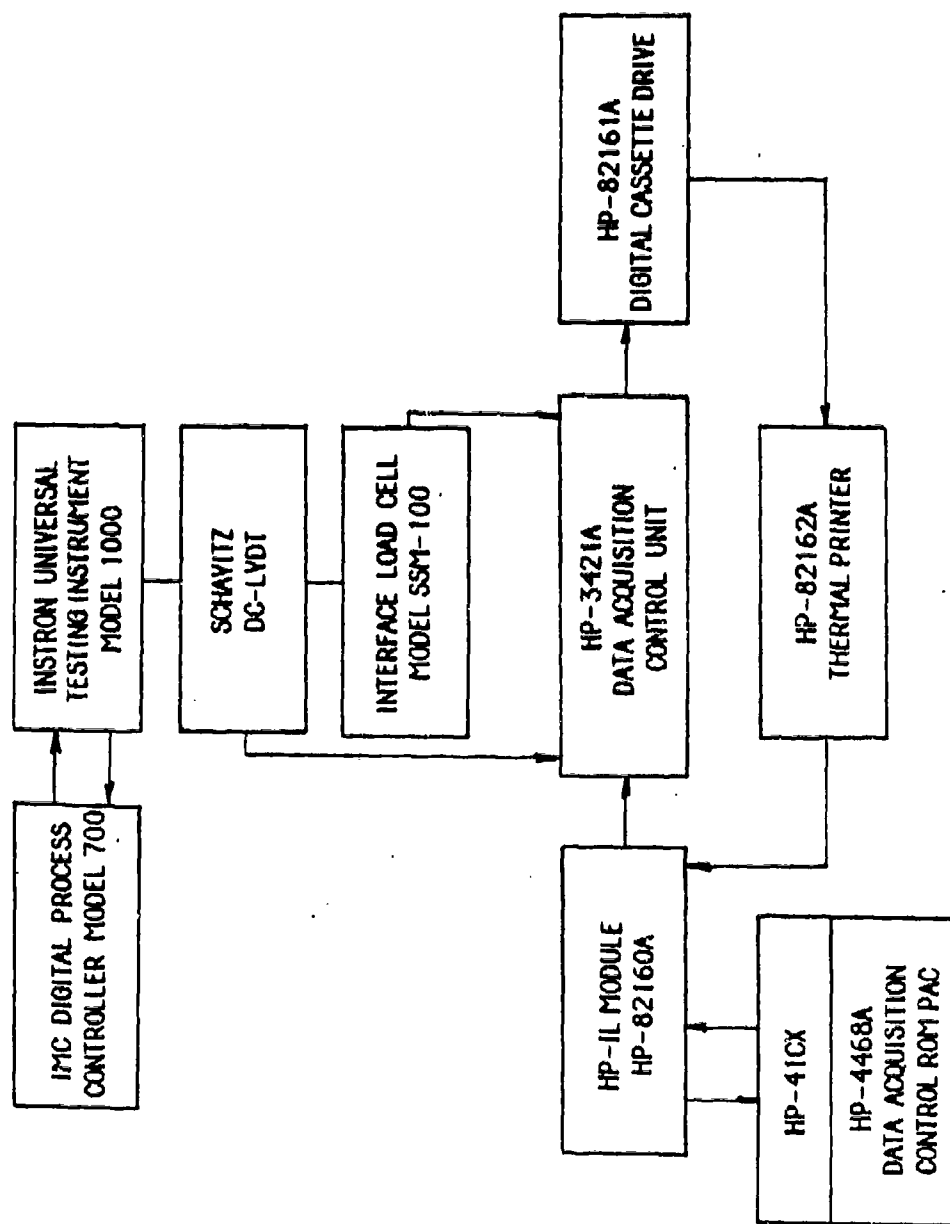


Figure 3.4. Block diagram of experimental setup.

block diagram of the instrumentation used. Its main feature is the IMC digital process controller. This processor (Figure 3.5) through automatic control of the movement of the Instron crosshead, using applied load as the control variable, creates a constant stress for a bundle with a variable number of fibers in time.

For a viscoelastic material the governing integral equation is

$$\sigma = \int_0^t (E(t - \tau) (d\epsilon/d\tau)) d\tau \quad (14)$$

If $E(t)$ were known, one could find $d\epsilon/d\tau$ and solve this equation for the desired stress σ . But the problem was, that this equation could not be solved in real time. Additionally it may not even be linear. The solution, was to let the material solve this equation, whether it was linear or not by using a specially prepared control sample.

The control sample was made from the same spool of graphite that the test samples were taken, and completely embedded in an epoxy resin. The reasoning behind this is the following: If a bare bundle of the same material were used as the controller, the compliance $J(t,n)$ which is a function of time and the number of fibers would change. However, with the matrix a broken fiber is not entirely lost because the load is transferred via the matrix binder and only a small ineffective length is lost. As a result $J(t,n)$ will not be affected because the number of fibers remains the same.

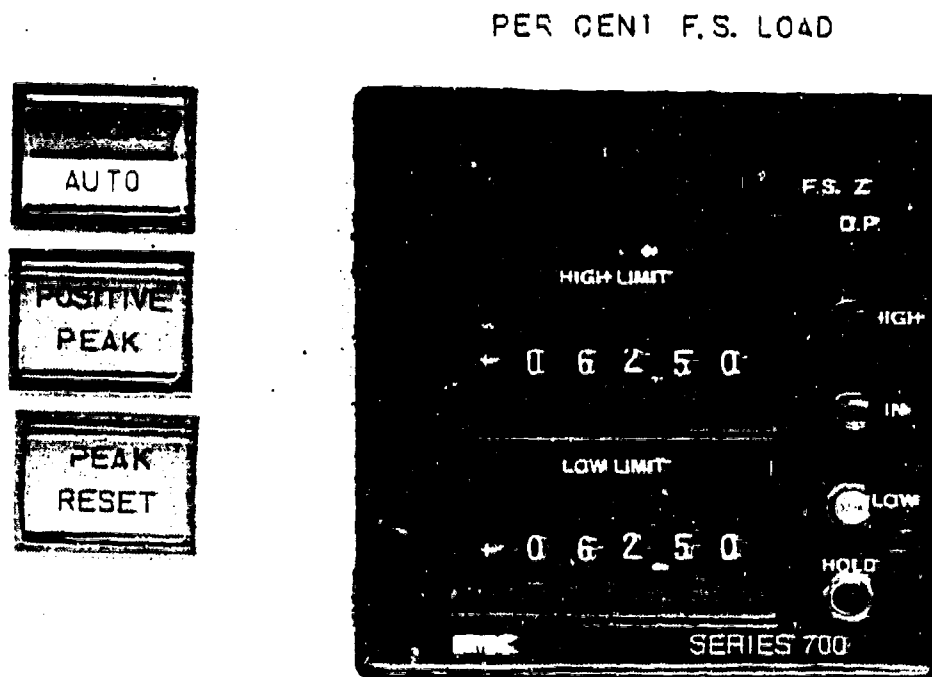


Figure 3.5. IMC digital processor/controller.

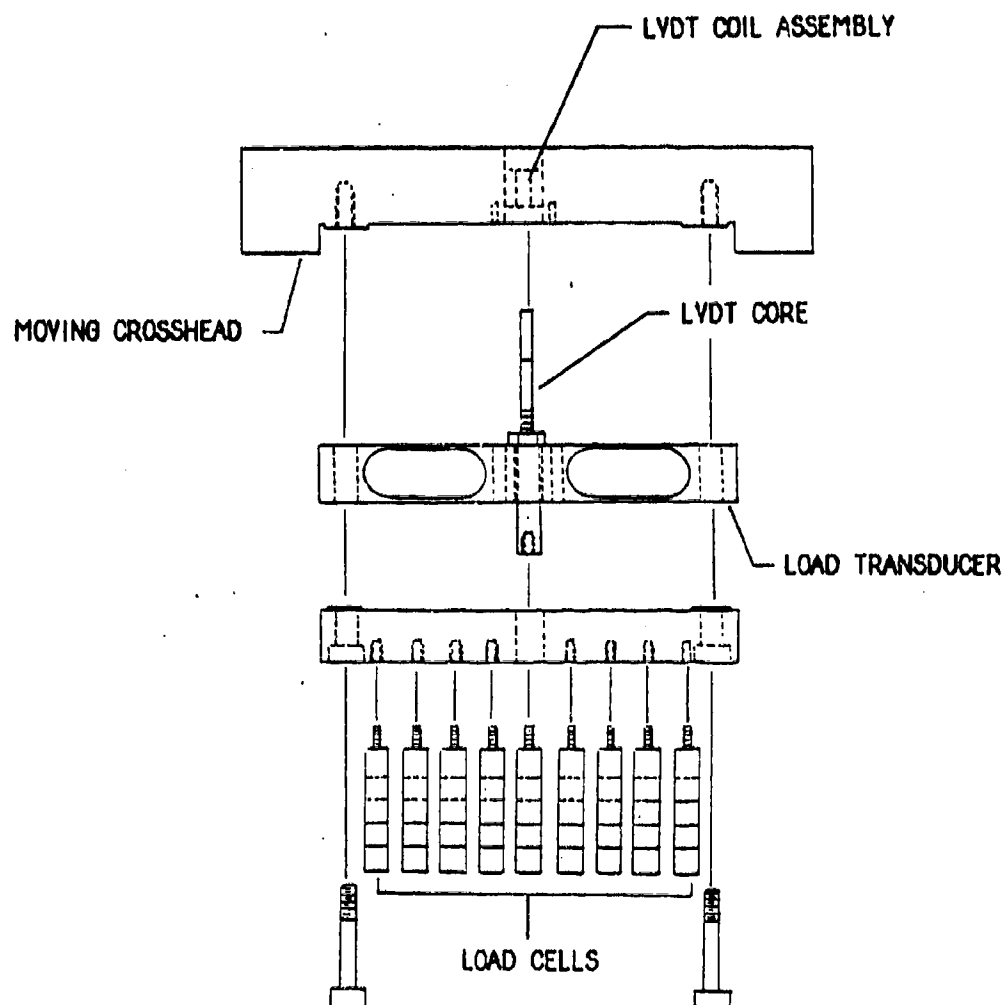


Figure 3.6. Moving crosshead with load transducer. LVDT coil assembly provides displacement information to the IMC digital processor.

There are provisions in the Instron crosshead for nine samples. The center position is for the control sample. At this position (Figure 3.6) the control sample is attached to an Interface SSM-100 load cell which is attached to a 100 pound load transducer. The output of the load transducer is fed into the IMC digital processor. By setting the desired maximum and minimum load on the face of the digital processor and activating the automatic mode, the crosshead will move under the control of the processor to the desired maximum setting and continually adjust to correct for the effects of creep, within the range set.

Because the crosshead is rigid, all the samples of the same length to the left and right of the control sample experiences the same displacement and the same strain. Thus each fiber of the same length in the sample are subjected to the same strain and therefore, the same stress.

C. DATA ACQUISITION

Data was recorded during the experiment using the Hewlett-Packard Interface Loop communications circuit (Figure 3.4). The HP-44468A Data Acquisition Control Pac provided the basic data logger software program. This program (Appendix A) was modified to permit the recording of time in hundredths of seconds, and edited to reduce the number of data registers used. It would have been desirable to have the HP-41CX calculator manipulate the data while sampling, by having a comparison made between consecutive readings of the same channel, to account for changes in voltage as a result of noise in the circuits. This was not feasible due to the design of the basic program and availability of data registers.

D. TESTING PROCEDURE

Prior to the beginning of the test the 100 pound load transducer was calibrated in accordance with the manufacturers instructions. The load cells were checked for linearity and repeatability in voltage output, and a reading was recorded, for a weight of 2 kilograms for each load cell.

For the first two experiments, three samples, one of which was the control sample and one of which was lubricated with silicone were placed into the Instron, in positions 6, 7, and 8 (Figure 3.7). The crosshead was raised just enough to remove the slack in the three samples. By the use of a specially designed differential screw mechanism (Figure 3.8) each sample was individually loaded to 2 kilograms. With each sample at the same load, the equal length requirement of the experiment was satisfied. The crosshead was then lowered to zero load and the samples rested for a period of one hour to erase any history of stress before beginning the test.

To start the experiment the IMC digital processors upper and lower limits were set to the prescribed load for that particular run. The crosshead control setting was adjusted to load the samples at the minimum rate possible. At the same time the loading was initiated, the data logger was activated.

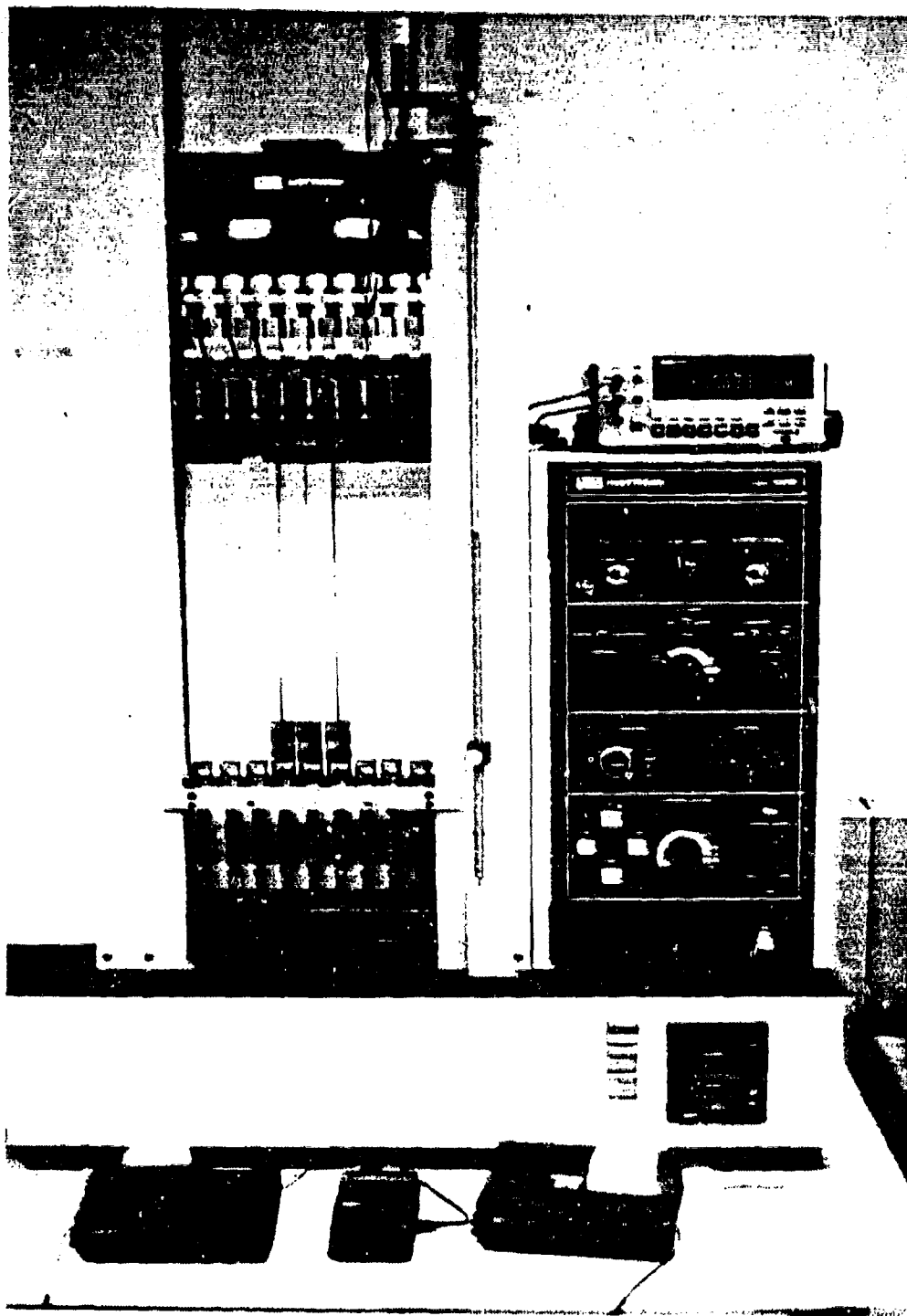


Figure 3.7. Test samples loaded in the Instron.

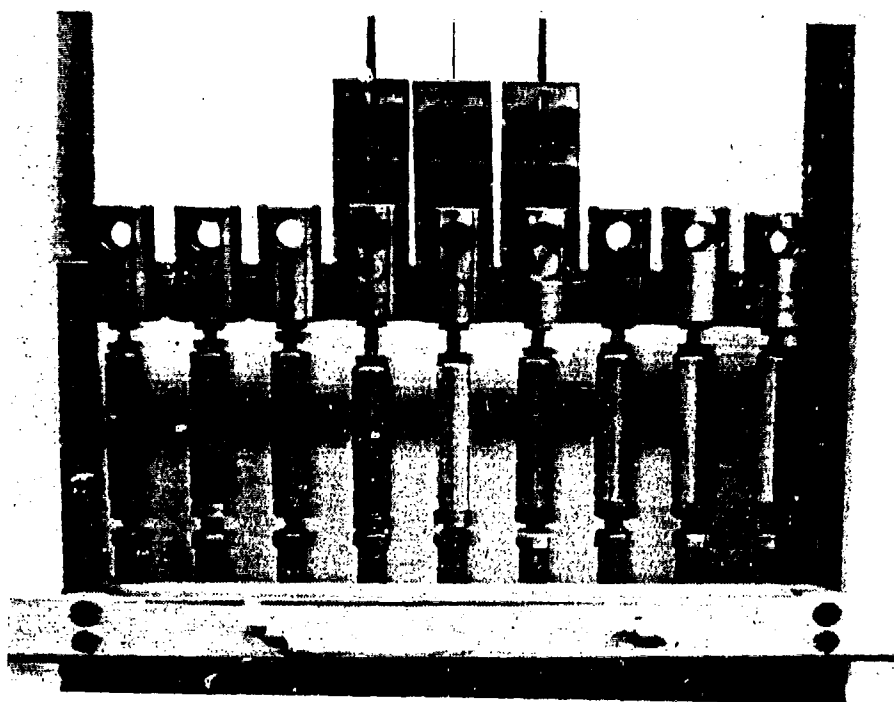


Figure 3.8. Differential screw mechanism is designed to give a displacement of 0.0045 inch per turn. The upper portion is threaded 10-32, the lower portion is threaded 1/4-28 and both are right handed.

IV. RESULTS

The experimental setup and procedure developed in this thesis produced acceptable initial results. However, the trial tests conducted have suggested that refinements in certain areas are necessary before actual testing begins.

The placing of the samples into the Instron machine, and loading each individual sample to the same load was straightforward. The differential screw mechanism functioned as designed, providing adequate resolution and adjustment range for the graphite samples tested. However, a differential screw of different thread ratios may be required for samples with a drastically different compliance, as a consequence of different fiber type or different gauge length.

The data acquisition rate was inadequate during the loading of the test samples at the start of the test. Installed in the HP-3421A data acquisition control unit were two 10 channel multiplexer boards, each with mechanical switching. The rate at which the unit switched from one channel to the next was fixed and relatively slow. During the initial loading sequence, it was important to obtain as many data points as possible in order to detect fiber breakage. In an attempt to compensate for the slow data acquisition rate the slowest possible setting on the Instron machine was used.

During the first test, the load was applied at 18 grams per second, which appeared to be too fast for the rate at which the data was being

recorded, but provided a reasonable continuous load increase on the specimens (Figure B.1). The effect of inter-fiber friction is noted, by comparing the loading curves for the lubricated and the nonlubricated samples between the time interval of 4 to 7 minutes. In the dry bundle, as the fibers failed and became entangled they produced local load concentrations which caused premature fiber breakage.

For the second test, the load was applied at a rate of 13 grams per second in an attempt to acquire more data points during the loading phase of the experiment. However, this was too slow, causing the drive motor of the Instron to stall as the load on the samples increased. The discontinuity in the load curves shown in Figure B.2a, for the first ten minute period resulted from the necessary readjustment of the loading rate on the Instron control panel in order to get the motor turning again.

The IMC digital processor performed as expected. It maintained the constant load required on the test samples as evidenced by the bundle control curves shown in Figure B.1, for time greater than 9 minutes, and in Figures B.2a and B.2b, for time greater than 12 minutes.

The effects of inter-fiber friction during creep rupture can be observed in Figures B.3 and B.4. The load supported by each individual bundle was normalized by their respective maximum loads attained at the peak of the loading ramp. As fibers fail as a result of stress rupture, which is the stress per fiber times the number of fibers, the total load decreases. The normalized curve of P/P_{\max} represents the percentage of failed fibers in time. In fact, it is the reliability function of the fiber. The silicone

lubricated bundle shows a continuous decrease in supported load suggesting that the fibers failed sequentially, as expected. On the other hand, the dry bundle shows large discontinuities in its curve suggesting that inter-fiber friction within the bundle, caused by entanglement among the failed fibers caused high local stress concentrations leading to an accelerated increase in the number of fiber failures.

During the constant load creep-rupture phase of the experiment, the time dependence of creep was physically observed by the operation of the IMC controller, causing the crosshead to move up in direction increasing displacement. The data recorded to support this observation was considered unreliable, in that it showed that the crosshead moved up and down. A polarity check of the LVDT and power supply used was conducted with no faults found. Had the excitation voltage been recorded, an explanation may have been possible.

From the results of the trial experiments, some insight into the time dependent failure of graphite is possible. There are three mechanistic views with regards to the time dependent life of graphite-epoxy. One hypothesized mechanism is that graphite fiber is not time dependent, it has basically infinite life. What limits the life of the composite, is that weak fibers are broken during loading. The composite is sustained from failure by matrix load sharing which transfers the load to neighboring fibers. For a viscoelastic matrix such as epoxy, the spatial dimension required to transfer a given load, increases with time, thereby increasing the ineffective length, exposing additional weaker fiber sites to stress

concentrations which in turn cause additional fiber failures. Therefore, the composite failure mechanism is by overload as a consequence of matrix creep.

Another hypothesis is that the fiber filament itself has time dependent strength. This time dependent strength may be caused by flaw growth within the fiber as a result of macro-viscoelastic creep, cumulated from micro-slip among graphite slip planes, or by random bond breakage activated by stress or temperature. In either case, the failure mechanism of the composite is by time-dependent flaw growth of the fiber.

Finally, the last hypothesis is that composite life is caused by both the viscoelastic deformation of the matrix and the time dependent flaw growth of the fiber.

The preliminary results of the trial experiments may provide definitive evidence towards the conformation of the correct failure mechanisms. The life test results of the graphite bundles are presented in Weibull coordinates in Figures B.5 and B.6. Under such representation, a single mechanism of failure for a weakest-link configuration would manifest itself in a straight line. The test sample subjected to the lower stress level is represented in Figure B.5. This figure shows an essentially linear increase in failure probability as a function of time. This suggests that at lower loads the function is unimodal, and that fiber life is time dependent. Whereas, for the test sample subjected to the higher stress level (Figure B.6), there are distinct discontinuities in the curve's slope occurring at 3 and 4.5 on the time scale, indicating that at higher loads the failure density function is multimodal. This would tend to imply not

only that graphite life is not infinite, but that flaw growth mechanisms by stress activation and flaw growth mechanisms by thermal (or time) activation are different. Further investigation confirming these observations would be important for the characterization of graphite fibers for use in high performance applications and to provide input toward the improvement of fiber manufacturing technologies.

V. CONCLUSIONS AND RECOMMENDATIONS

A. CONCLUSIONS

The experimental procedure presented proved to be a suitable method for lifetime testing of graphite bundles under constant load. The preliminary results of the trial experiments suggest that graphite life is time dependent and that the failure mechanism of flaw growth produced by temperature or time is distinct from that which is produced by stress. Through further refinement, the experimental technique developed offers promise of increased understanding of the failure processes.

B. RECOMMENDATIONS

The following are given as recommendations to improve the accuracy of the data.

1. *Data Acquisition:* Insert the HP-85 data logging system into the HP-IL loop for the initial loading of the bundles. This unit can record data at a much faster rate.
2. *Sample Preparation:* Lubricate the test samples with silicone oil to eliminate the catastrophic effects of inter-fiber friction.
3. *Procedure:* Load the samples at a minimum of 18 grams per second. This rate will prevent the drive motor from stalling.

APPENDIX A

PROGRAM LISTING

DATA LOGGER

```

01 LBL "LOGM"
02 SF 10
03 GTO 35
04 LBL "DLM"
05 CF 10
06 LBL 35
07 SF 12
08 SF 27
09 " HP 3421A"
10 AVIEW
11 CLKY
12 "DATA LOGGER"
13 AVIEW
14 CF 12
15 "DLM"
16 32
17 AK
18 "CLKY"
19 -32
20 AK
21 "LOG"
22 35
23 AK
24 CF 13
25 RCL 35
26 ENTER
27 INT
28 X=Y?
29 GTO 31
30 X<>Y
31 FRC
32 1 E3
33 *
34 STO 35
35 LBL 31
36 "NEW ? Y/N"
37 AON
38 FC? 10
39 PROMPT
40 AOFF
41 ASTO Y
42 "Y"
43 ASTO X

```

```

44 X=Y
45 GTO 01
46 "EDIT ? Y/N"
47 AON
48 FC? 10
49 PROMPT
50 CF 10
51 AOFF
52 ASTO X
53 "Y"
54 ASTO Y
55 X=Y?
56 GTO 04
57 SF 12
58 "-*-EDITOR-*-"
59 AVIEW
60 CF 12
61 GTO 18
62 LBL F
63 "DCV"
64 AVIEW
65 1
66 GTO 02
67 LBL 02
68 1 E2
69 +
70 1 E-7
71 *
72 RCL 05
73 +
74 ISG 35
75 ABS
76 SF 25
77 RCL IND 35
78 FS?C 25
79 GTO 10
80 DSE 35
81 ABS
82 "OUT OF ROOM"
83 AVIEW
84 PSE
85 FS? 10
86 GTO 16

```

```

87 GTO 04
88 LBL 10
89 RDN
90 FS? 10
91 GTO 21
92 STO IND 35
93 GTO 03
94 LBL 21
95 STO 04
96 RCL 06
97 39
98 +
99 STO 08
100 1 E-3
101 *
102 RCL 35
103 1
104 -
105 STO 07
106 LASTX
107 +
108 +
109 STO 06
110 LBL 22
111 RCL IND 07
112 STO IND 06
113 DSE 07
114 ABS
115 DSE 06
116 GTO 22
117 RCL 04
118 STO IND 08
119 RCL 08
120 INT
121 38
122 -
123 STO 06
124 GTO 03
125 LBL 01
126 CLX
127 STO 30
128 37
129 STO 35

```

Figure A.1. Modified HP44468A Data Logger Routine

130 LBL 03	178 "USER"	226 X=Y?
131 FIX 0	179 ARCL X	227 SF 08
132 CF 29	180 AVIEW	228 SF 21
133 "FIRST CH?"	181 16	229 FC? 08
134 CF 22	182 +	230 CF 21
135 AOFF	183 GTO 02	231 "PRINT"
136 PROMPT	184 LBL 04	232 FC? 08
137 FC? 22	185 FS? 10	233 "I-OFF"
138 GTO 04	186 GTO 16	234 AVIEW
139 ENTER	187 37	235 LBL 06
140 "LAST CH?"	188 RCL 35	236 AOFF
141 PROMPT	189 X<=Y?	237 SF 29
142 CLA	190 STOP	238 SF 28
143 ARCL Y	191 1 E-3	239 XROM "ALM"
144 "I-- "	192 +	240 X<0?
145 ARCL X	193 38	241 GTO 05
146 AVIEW	194 +	242 PWRDN
147 1000	195 STO 35	243 OFF
148 /	196 CF 09	244 LBL 05
149 +	197 "RECORD Y/N"	245 XEQ "DLMLM"
150 STO 05	198 CF 23	246 ISG 32
151 CF 23	199 AON	247 GTO 29
152 "FUNCTION?"	200 PROMPT	248 1
153 PROMPT	201 CF 20	249 "I"
154 FS? 23	202 FC?23	250 SF 25
155 GTO 19	203 SF 20	251 CLAL
156 "PRESS FN KEY"	204 ASTO Y	252 CF 25
157 PROMPT	205 "Y"	253 PWRDN
158 LBL 19	206 ASTO X	254 OFF
159 CF 22	207 X=Y?	255 LBL 29
160 "USER0-83 ?"	208 SF 09	256 RCL 34
161 PROMPT	209 "RECORD"	257 X=0?
162 FS? 22	210 FC? 09	258 GTO 05
163 GTO 20	211 "I-OFF"	259 PWRDN
164 "LAST SETUP"	212 AVIEW	260 OFF
165 AVIEW	213 FC? 55	261 GTO 05
166 PSE	214 GTO 06	262 OFF
167 "NOT STORED"	215 "PRINT? Y/N"	263 LBL 18
168 AVIEW	216 CF 23	264 SF 10
169 PSE	217 AON	265 CF 29
170 GTO 03	218 PROMPT	266 FIX 0
171 LBL 20	219 CF 21	267 36
172 INT	220 FC? 23	268 RCL 35
173 ABS	221 SF 21	269 X<=Y?
174 84	222 ASTO Y	270 37
175 X<=Y?	223 "Y"	271 STO 35
176 GTO 19	224 LAST X	272 LBL 16
177 RDN	225 CF 08	273 "COMMAND ?"

Figure A.1. Modified HP44468A Data Logger Routine (cont'd)

274 AON	322 RCL 35	370 GTO 16
275 PROMPT	323 X<>Y	371 STO 02
276 AVIEW	324 X>Y?	372 FIX 0
277 ASTO X	325 GTO 13	373 1 E-3
278 "LIST"	326 X=Y?	374 *
279 ASTO Y	327 GTO 36	375 38
280 X=Y?	328 X<>Y	376 +
281 GTO 07	329 1	377 STO 35
282 "INSERT"	330 -	378 LBL 08
283 ASD Y	331 1 E-3	379 RCL IND 35
284 X=Y?	332 *	380 STO 01
285 GTO 09	333 +	381 XROM "DECODE"
286 "DELETE"	334 STO 06	382 ASTO 00
287 ASTO Y	335 LBL 15	383 CLA
288 X=Y?	336 RCL 06	384 RCL 35
289 GTO 12	337 1	385 INT
290 "END"	338 +	386 38
291 ASTO Y	339 RCL IND X	387 -
292 X=Y?	340 STO IND 06	388 ARCL X
293 GTO 17	341 ISG 06	389 "1-: "
294 "HELP"	342 GTO 15	390 RCL IND 35
295 ASTO Y	343 LBL 36	391 ENTER
296 X=Y?	344 DSE 35	392 INT
297 GTO 14	345 ABS	393 ARCL X
298 "INVALID CMD"	346 GTO 16	394 RDN
299 AVIEW	347 LBL 14	395 FRC
300 PSE	348 "LIST"	396 1 E3
301 GTO 16	349 AVIEW	397 *
302 LBL 17	350 PSE	398 INT
303 "*END EDITOR*"	351 "INSERT"	399 "1--"
304 AVIEW	352 AVIEW	400 ARCL X
305 PSE	353 PSE	401 "1-, "
306 CF 10	354 "DELETE"	402 ARCL 00
307 GTO 04	355 AVIEW	403 AVIEW
308 LBL 12	356 PSE	404 ISG 35
309 CF 22	357 "END"	405 GTO 08
310 "NUMBER ?"	358 AVIEW	406 RCL 02
311 AOFF	359 PSE	407 STO 35
312 PROMPT	360 GTO 16	408 GTO 16
313 FC? 22	361 LBL 13	409 LBL 09
314 GTO 16	362 "NONEXISTENT"	410 CF 22
315 INT	363 AVIEW	411 AOFF
316 ABS	364 PSE	412 "AFTER NUMR ?"
317 "DELETE"	365 GTO 16	413 PROMPT
318 ARCL X	366 LBL 07	414 FC? 22
319 AVIEW	367 37	415 GTO 16
320 38	368 RCL 35	416 X<0?
321 +	369 X<=Y?	417 -1

Figure A.1. Modified HP44468A Data Logger Routine (cont'd)

```
418 RCL 35
419 38
420 -
421 X<>Y
422 X>Y?
423 GTO 13
424 STO 06
425 "AFTER "
426 ARCL X
427 AVIEW
428 GTO 03
429 END
```

Figure A.1. Modified HP44468A Data Logger Routine (con'd)

DATA LOGGER OUTPUT FORMAT

01 LBL "DLMLM"	48 ADATE	95 CF 10
02 "C"	49 TIME	96 ISG 01
03 CF 29	50 STO 01	97 GTO 04
04 FC? 08	51 FIX 6	98 CLA
05 CF 21	52 ATIME	99 FIX 0
06 RCL 35	53 FC? 08	100 ARCL 32
07 STO 01	54 AVIEW	101 RCL 33
08 2	55 PRA	102 FS? 09
09 LBL 10	56 ADV	103 SEEKR
10 3	57 .001	104 RCL IND 35
11 +	58 FS? 09	105 STO 01
12 RCL IND 01	59 WRTRX	106 RCL 37
13 ENTER	60 2	107 ST+ 33
14 FRC	61 STO 33	108 1
15 1 E3	62 CF 10	109 -
16 *	63 LBL 02	110 1 E3
17 INT	64 RCL IND 35	111 /
18 X<>Y	65 STO 01	112 FS? 09
19 INT	66 XROM "DECODE"	113 WRTRX
20 -	67 ASTD 00	114 ADV
21 +	68 ASHF	115 ISG 35
22 ISG 01	69 ASTD 36	116 GTO 02
23 GTO 10	70 2	117 RCL 35
24 FIX 0	71 STO 37	118 FRC
25 CLA	72 LBL 04	119 38
26 ARCL 32	73 FIX 0	120 +
27 FC? 09	74 CLA	121 STO 35
28 GTO 03	75 RCL 01	122 RTN
29 SF 25	76 XEQ IND 36	123 END
30 CREATE	77 FS?C 10	
31 FS?C 25	78 ASTD 00	
32 GTO 03	79 STO IND 37	
33 PURGE	80 CLA	
34 CREATE	81 RCL 01	
35 LBL 03	82 INT	
36 "PASS "	83 ARCL X	
37 ARCL 32	84 RCL IND 37	
38 AVIEW	85 ISG 37	
39 CLA	86 SIGN	
40 ARCL 32	87 "I-: "	
41 0	88 ENG 5	
42 FS? 09	89 ARCL X	
43 SEEKR	90 "I- "	
44 CLA	91 ARCL 00	
45 DATE	92 FC? 08	
46 STO 00	93 AVIEW	
47 FIX 4	94 PRA	

Figure A.2. Modified HP44468A Output Format Routine

APPENDIX B

GRAPHICAL RESULTS

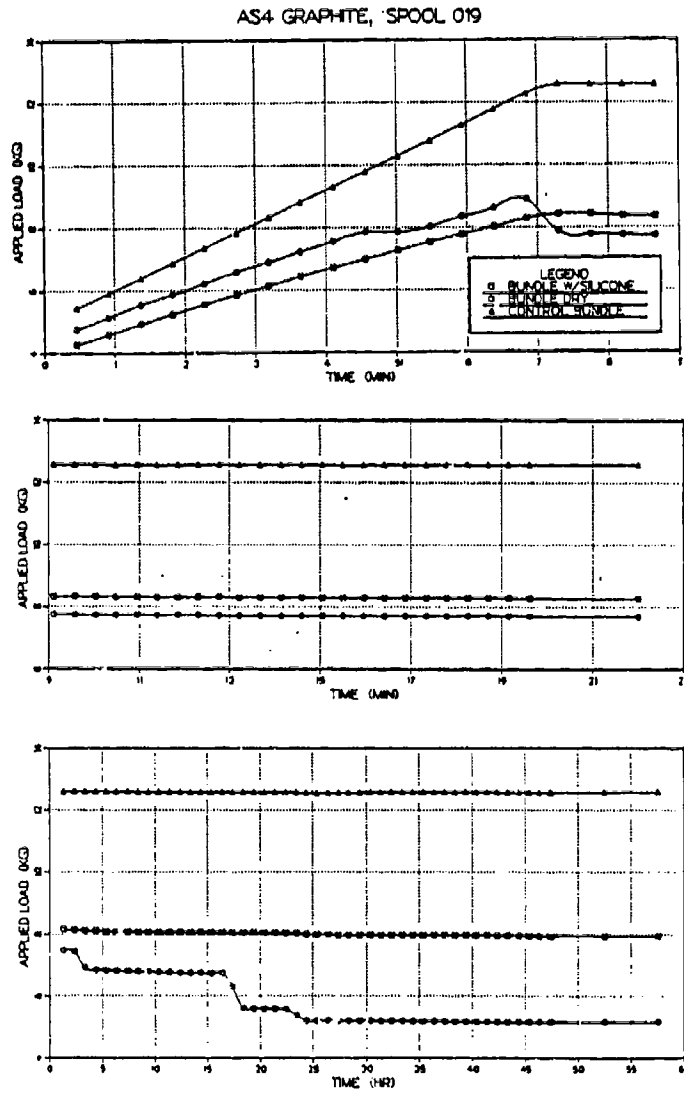


Figure B.1. Test 1: Load-Time curves. Maximum constant load on the control sample was 12.575 kilograms.

AS4 GRAPHITE, SPOOL 019

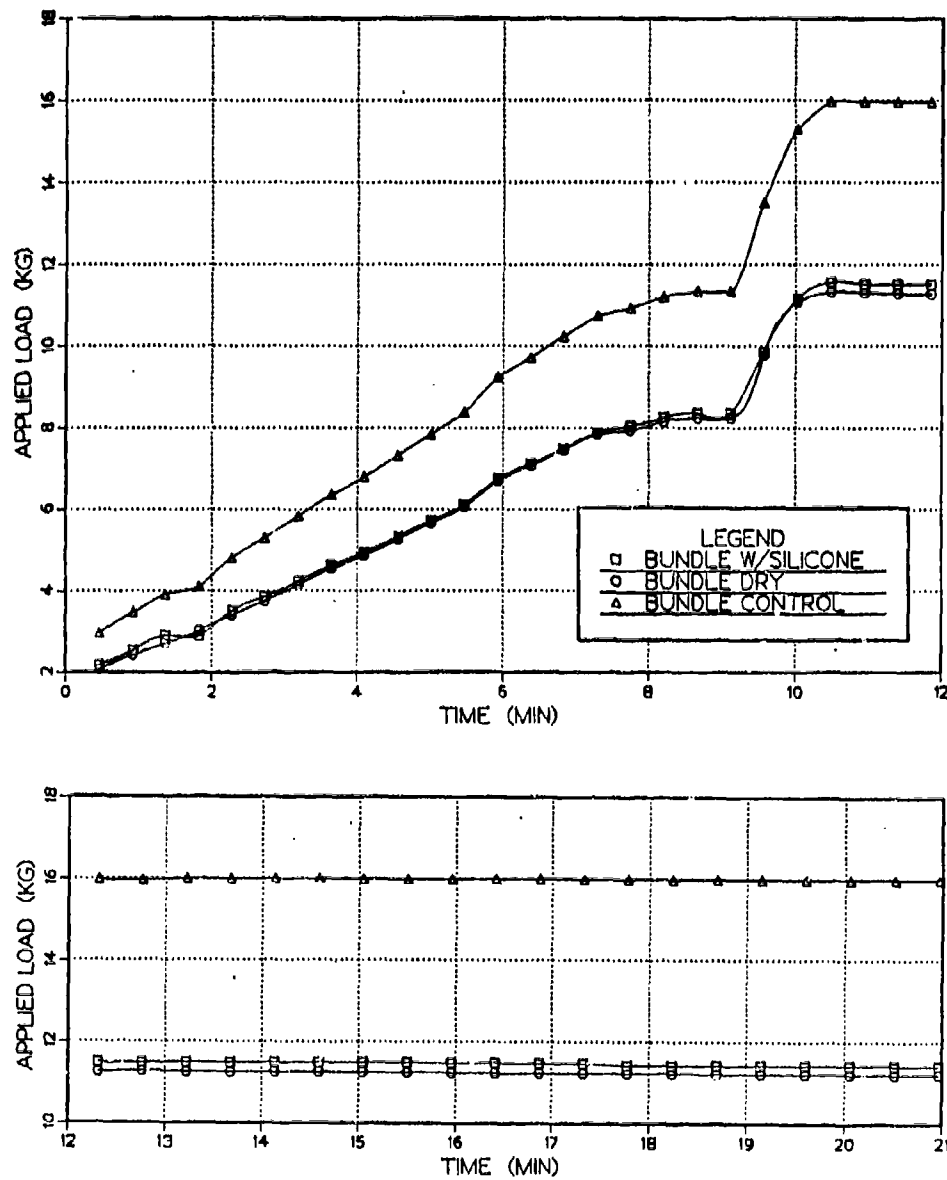


Figure B.2a. Test 2: Load-Time curves. Maximum constant load on the control sample was 16.003 kilograms.

AS4 GRAPHITE, SPOOL 019

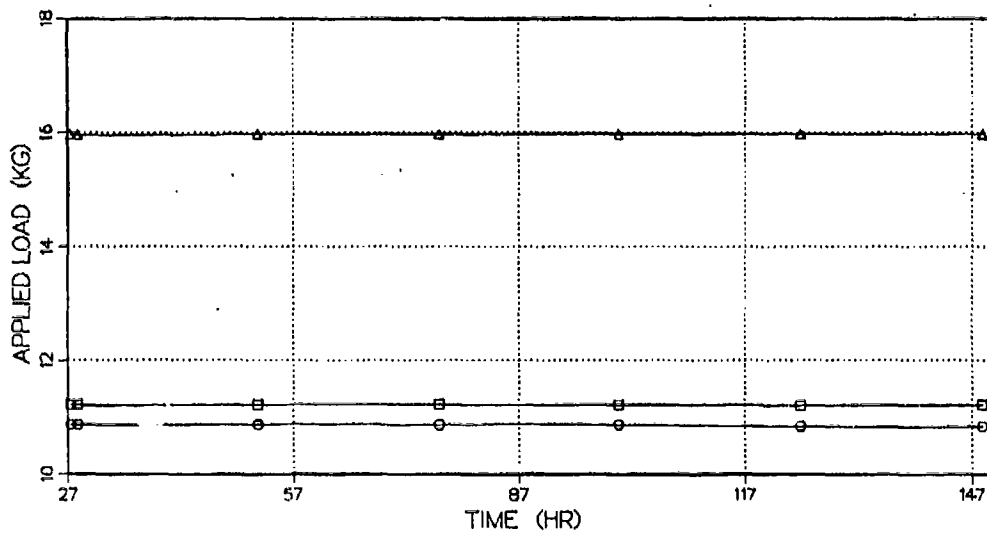
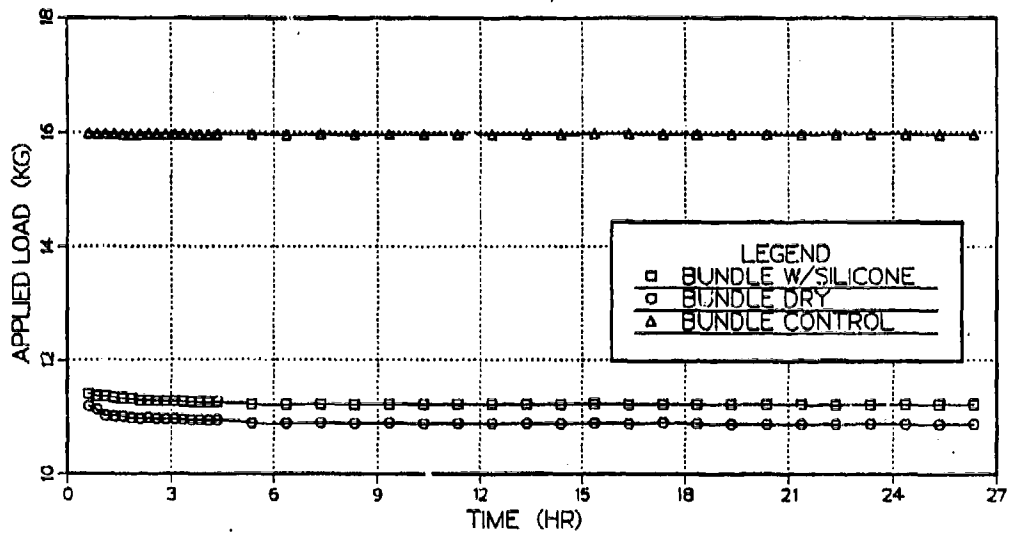


Figure B.2b. Continuation of Test 2: Load-Time curves.

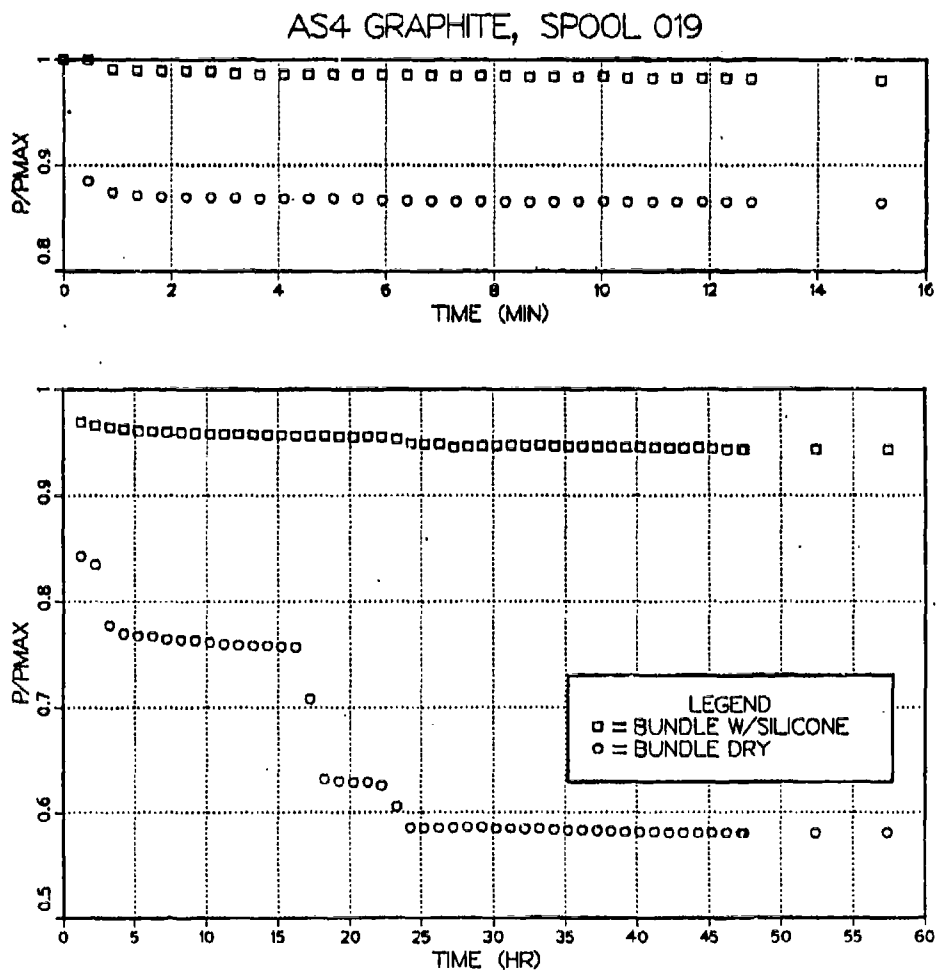


Figure B.3. Test 1: Normalized load curves. Maximum load achieved by the bundle with silicone was 8.430 kilograms. Maximum load achieved by the dry bundle was 8.900 kilograms.

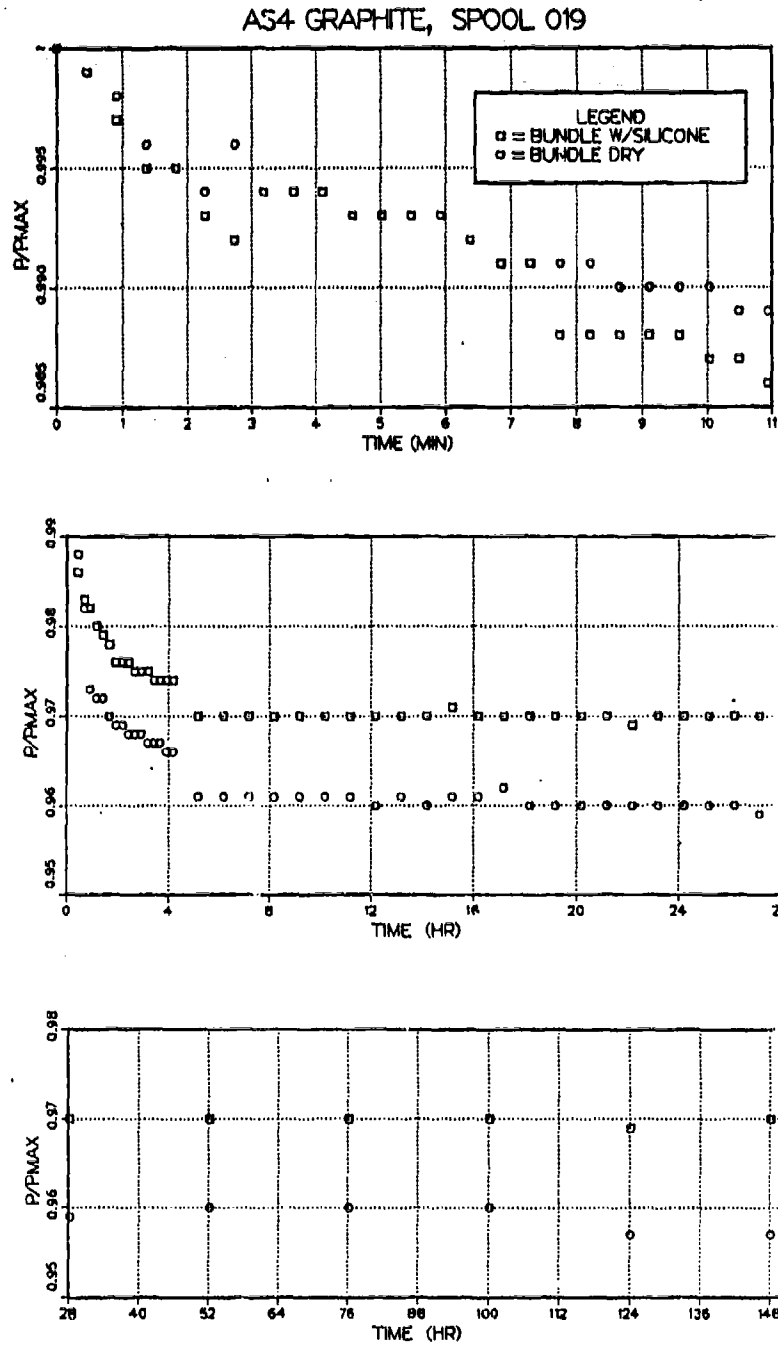


Figure B.4. Test 2: Normalized load curves. Maximum load achieved by the bundle with silicone was 11.572 kilograms. Maximum load achieved by the dry bundle was 11.329 kilograms.

AS4 GRAPHITE, SPOOL 019

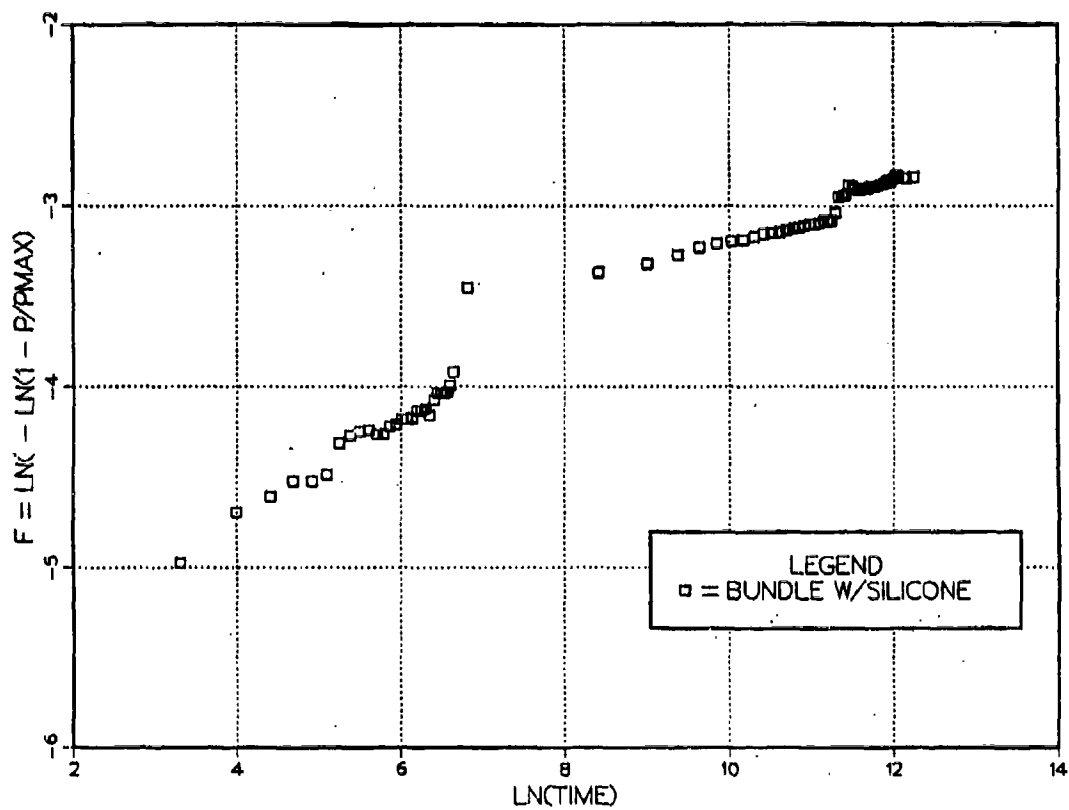


Figure B.5. Test 1: Lifetime distribution curve.

AS4 GRAPHITE, SPOOL 019

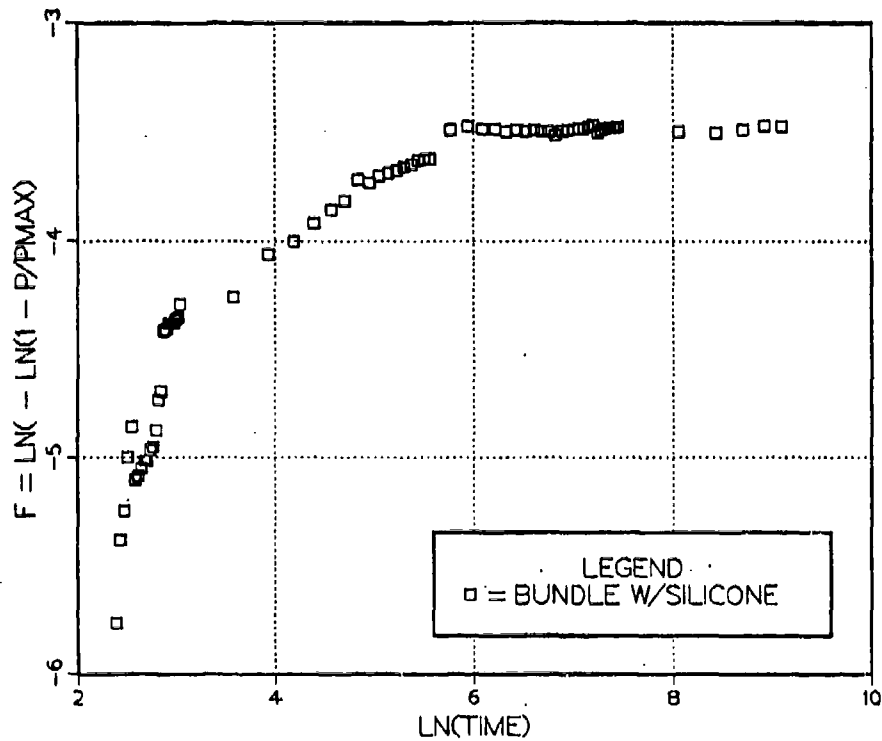


Figure B.6. Test 2: Lifetime distribution curve.

LIST OF REFERENCES

1. Tsai, S. W., *Composites Design-1985*, Think Composites, 1985.
2. Rosen, W. B., "Tensile Failure of Fibrous Composites," *AIAA Journal*, Vol. 2, No. 11, November 1964.
3. Rosen, W. B., "Mechanics of Composite Strengthening," *Fiber Composite Materials*, American Society for Metals, 1965.
4. Wu, E. M., Class notes for Naval Postgraduate School Course AE. 4103, "Advanced Aircraft Structures," 1985.
5. Phoenix, S. L., and E. M. Wu, *Statistics for the Time Dependent Failure of Kevlar 49/Epoxy Composites: Micromechanical Modeling and Data Interpretation*, UCRL-53365, Lawrence Livermore Nation Laboratory, Livermore, California, 1983.
6. Wagner, H. D., P. Schwartz, and S. L. Phoenix, *Lifetime Statistics for Single Kevlar 49 Filaments in Creep Rupture*, Cornell University, 1985.

BIBLIOGRAPHY

Jones, R. M., *Mechanics of Composite Materials*, McGraw-Hill, 1975.

Piggott, M. R., *Load Bearing Fiber Composites*, Pergamon Press, 1980.

Smith, C. O., *Introduction to Reliability in Design*, Robert E. Krieger Co., 1983.

INITIAL DISTRIBUTION LIST

	No. Copies
1. Defense Technical Information Center Cameron Station Alexandria, Virginia 22304-6145	2
2. Library, Code 0142 Naval Postgraduate School Monterey, California 93943-5002	2
3. Department Chairman, Code 67 Department of Aeronautics Naval Postgraduate School Monterey, California 93943-5002	1
4. Prof Edward M. Wu, Code 67-WT Department of Aeronautics Naval Postgraduate School Monterey, California 93943-5002	2
5. LT Fred D. Carozzo, Jr 18F Polk Avenue Clairton, Pennsylvania 15025	2